INL/CON-05-00460
PREPRINT

Equilibrium Model for Ion Exchange Between Multivalent Cations and Zeolite-A in a Molten Salt

AIChE Annual Conference 2005

Supathorn Phongikaroon
Michael F. Simpson

October 2005

The INL is a
U.S. Department of Energy
National Laboratory
operated by
Battelle Energy Alliance

Equilibrium Model for Ion Exchange Between Multivalent Cations and Zeolite-A in a Molten Salt

Supathorn Phongikaroon and Michael F. Simpson
Pyroprocessing Technology Dept., Fuel Cycle Programs Div., Idaho National Laboratory, Idaho Falls, ID 83403

A two-site equilibrium model that previously only accommodated monovalent cations has been extended to include divalent and trivalent cations for ion exchange between zeolite-A and molten chloride salts, a process being considered for concentrating nuclear fission products into high level waste forms. Equilibrium constants were determined by fitting the model to equilibrium data sets for ion exchange between zeolite-A and Cs ternary salt (CsCl-LiCl-KCl), Rb ternary salt (RbCl-LiCl-KCl), Na ternary salt (NaCl-LiCl-KCl), Sr ternary salt ($SrCl_2$-LiCl-KCl), and U ternary salt (UCl_3-LiCl-KCl). The results reveal a good fit between the experimental data sets and the model. The two ion exchange sites, framework sites and occluded sites, demonstrate different relative selectivities for the cations. It was found that Sr^{2+} is the preferred cation in the ion exchange site, and Cs^+ is the preferred cation in the occlusion site. Meanwhile, Li^+ has the highest combined selectivity when both ion exchange and occlusion sites are considered. Interestingly, divalent and trivalent species are more preferred in the ion exchange site than the monovalent species with the exception of Li^+.

Key words: ion exchange, zeolite, molten salt, pyroprocessing, separation

Introduction

Spent fuel from the Experimental Breeder Reactor-II (EBR-II) is currently being treated in electrorefiners at the Idaho National Laboratory (INL) in a process known as pyroprocessing of spent nuclear fuel. In electrorefining, uranium is oxidized at the anode while simultaneously being reduced and deposited at the cathode.[1,2] Plutonium, sodium, and fission products are oxidized to form chlorides in the electrolyte, which consists primarily of eutectic LiCl-KCl along with UCl_3. The overall objective of pyroprocessing is to separate reusable uranium from fission products, which can be placed into waste forms for long-term storage in a geological repository. The spent electrolyte, consisting of LiCl, KCl, NaCl, various actinide chlorides, and various fission product chlorides, must be periodically removed from the electrorefiner and combined with zeolite-4A (LTA) and glass to form a ceramic waste form. The expected composition of waste electrorefiner salt after treatment is given in Table 1. Currently, methods are being investigated for chemically reducing the actinide chlorides prior to combining the salt with the zeolite to prevent the actinides from being discarded in the ceramic waste stream. In the baseline process, excess zeolite-4A is used so that all of the salt is absorbed into its alpha cages. However, this is seen as a wasteful approach, since useful LiCl-KCl is thrown away in addition to the NaCl and fission product chlorides.[3] If a selective ion exchange material existed, waste volume reduction could potentially be realized. An ion exchange process has, thus, been proposed for minimizing ceramic waste volume generated from the pyroprocessing method for treating spent nuclear fuel. One viable approach is that a zeolite ion exchange column could be implemented to remove any contaminants

Correspondence concerning this article should be addressed to S. Phongikaroon at supathorn.phongikaroon@inl.gov.

Table 1. Composition of Waste Electrorefiner Salt After Treatment

Composition (mol%)			
LiCl (36.12)	$SrCl_2$ (0.57)	$NdCl_3$ (1.48)	$PuCl_3$ (1.05)
KCl (26.13)	UCl_3 (0.59)	$PmCl_3$ (0.02)	$AmCl_3$ (0.003)
NaCl (29.35)	$BaCl_2$ (0.58)	$SmCl_3$ (0.28)	$PrCl_3$ (0.44)
RbCl (0.26)	$LaCl_3$ (0.47)	$EuCl_3$ (0.02)	YCl_3 (0.34)
CsCl (1.37)	$CeCl_3$ (0.89)	$GdCl_3$ (0.01)	$NpCl_3$ (0.03)

from the LiCl-KCl and allow the cleaned salt to be recycled back to the electrorefiner.[4]

For such an ion exchange process, zeolite-A has been proposed to selectively remove fission products from the LiCl-KCl based electrolyte. For this reason, the nature of the interactions between various molten chloride salts and zeolite-A is of great interest. And predictive information is necessary to help design and optimize an ion exchange process. In general, two processes occur when molten salts and zeolite come into contact: (1) molten salt occlusion to form salt-loaded zeolite, and (2) ion exchange between the molten salt and salt-loaded zeolite.[5]

Previous work on modeling equilibrium ion exchange between zeolite-A and molten chloride salts has involved two different types of models that fit well with experimental data for monovalent species.[6,7] The approach taken by Lexa and Johnson[6] was strictly empirical and based on simple geometrical arguments, limited zeolite cage volume versus involved ionic radii; while the approach taken by Simpson and Gougar[7] was based on balancing the adsorption and desorption rates from two different types of sites in the zeolite. Neither approach was encumbered with the complexity that considering divalent and trivalent species involves. Each such species occupies two or three sites, respectively.

Despite the complexity described above, Gougar[8] has derived a model that accounts for divalent and trivalent cations while avoiding mathematical complexity. In this study, cesium and neodymium were studied as surrogate fission species. The model was derived from an analogy of probability through reaction kinetics and expressed in a one-dimensional domain. The resulting model presented therein revealed a decent fit to experimental data.

The main scope of this study was to extend the modeling approach originally proposed by Simpson and Gougar[7] for monovalent species to include divalent and trivalent cations, using the same fundamental approach. The principal challenge was to derive such a model that was sufficiently sophisticated to capture a realistic mechanism for ion exchange while still being simplistic enough to fit to available data without having to revert to complicated numerical solution methods.

Model Development

A fully hydrated zeolite-A pseudo unit cell will have 24 tetrahedra (12 AlO_4 and 12 SiO_4) and 27 water molecules.[5,9] Breck[5] has provided a diagram of zeolite-A showing that the smallest pore diameter has a size of 0.42 nm, which leads into a larger cavity of minimum free diameter of 1.14 nm. The cavity is surrounded by 8 truncated octahedra connected by their square faces in a cubic structure. Generally speaking, it is 8× pseudo unit cell for the true cell. In many chemical processes and analyses, the typical pseudo cell of zeolite-A is conventionally expressed as follows:

$$M_{12/n_i}^{(n_i)^+}(AlO_2)_{12}(SiO_2)_{12} \tag{1}$$

where $M^{(n_i)^+}$ refers to framework charge-balancing cations, and n_i is the charge of the exchangeable cation i. Eq. 1 indicates that there are possibly numerous combinations of multivalent cations that can balance the negative charge from Al in this tetrahedral framework. A representative but not comprehensive list of such cations is provided in Table 2 with their ionic radii and chemical potentials.[5,6] From this idea, it is more convenient to use mole equivalents for calculating the concentration within the zeolite phase, where there are 12 mole equivalent ion exchange sites per mole of pseudo unit cells. This value (θ_i) is calculated based on the following formula:

$$\theta_i = \frac{12 \times [n_i \times (\text{wt}\%_i)/MW_i]}{[(\text{wt}\%_{Al})/MW_{Al}]} \tag{2}$$

where $\text{wt}\%_i$ is the weight percent of species i and MW_i is the molecular weight of species i in the zeolite.

In a multicomponent system, there are many possible ion exchange reactions, which makes the task of modeling the entire system difficult. A great deal of simplification can be realized by using a reference cation and defining all ion exchange reactions as involving this reference cation.

$$(M_i^{(n_i)^+})_S + n_i(Li^+)_Z \leftrightarrow (M_i^{(n_i)^+})_Z + n_i(Li^+)_S \tag{3}$$

In Eq. 3, the subscripts S and Z denote the salt and zeolite phases, respectively. Li is the reference species for every reaction. For example, if there is an exchange between Cs^+ and K^+ cation ions, then this can be represented like a chain by exchanging both Cs^+ with Li^+ and K^+ with Li^+. This approach is valid when only the equilibrium of the system is of concern, not the kinetics. But it provides an advantage by keeping the mathematical derivation simple and solvable. From Eq. 3 both forward and reverse reaction rates can be derived as follows:

$$\begin{aligned} r_{f,i} &= k_{f,i}x_i(y_{Li})^{n_i} \\ r_{r,i} &= k_{r,i}y_i(x_{Li})^{n_i} \end{aligned} \tag{4}$$

where $k_{f,i}$ is the forward rate constant of species i, $k_{r,i}$ is the reverse rate constant of species i, x_i is the mole fraction of

Table 2. List of the Framework Cations and Their Ionic Radii and Chemical Potentials

i	M	n_i	Ionic Radius (nm)	Chemical Potential (kJ/mol)
1	Cs	1	0.169[a]	$CsCl = -6.5 \pm 0.5$[c]
2	Na	1	0.095[a]	$NaCl = -0.0 \pm 0.5$[c]
3	Li	1	0.060[a]	—
4	K	1	0.133[a]	—
5	Rb	1	0.148[a]	$RbCl = -0.4 \pm 0.5$[c]
6	Sr	2	0.132[b]	$SrCl_2 = -84.0 \pm 0.1$[b]
7	U	3	0.117[b]	$UCl_3 = -101.1 \pm 0.2$[b]

[a]The values are obtained from Ebbing DD. *General Chemistry*. Boston: Houghton Mifflin Company; 1996: 352-353.
[b]The values are obtained from Ref. [10].
[c]The values are obtained from Ref. [6].

species i in the salt phase, and y_i is the moles of species i per mole of zeolite pseudo unit cells (in the zeolite phase). In a system at equilibrium, both reaction rates should be considered equal, and the loading of species i in the zeolite can be solved:

$$y_i = \left(\frac{k_{f,i}}{k_{r,i}}\right)\left(\frac{x_i}{(x_{\mathrm{Li}})^{n_i}}\right)(y_{\mathrm{Li}})^{n_i} = K_i\left(\frac{x_i}{(x_{\mathrm{Li}})^{n_i}}\right)(y_{\mathrm{Li}})^{n_i} \qquad (5)$$

where K_i is a dimensionless equilibrium constant. For example, for strontium (Sr), Eq. 5 would be written as:

$$y_{\mathrm{Sr}} = K_{\mathrm{Sr}}\left(\frac{x_{\mathrm{Sr}}}{(x_{\mathrm{Li}})^2}\right)(y_{\mathrm{Li}})^2. \qquad (6)$$

As mentioned above, there are interactions occurring in two types of sites within the zeolite—(1) ion exchange sites, where the cation charge is balanced by the negative charge in the framework of zeolite-A; and (2) occlusion sites, where whole salt molecules are occluded in alpha cages via space filling. This implies that each site will have a different affinity for the cations and that two sets of K_i values will be needed for the model. Therefore, Eq. 5 can be expressed for both types of sites within the zeolite by:

$$y_i^{\mathrm{IX}} = K_i^{\mathrm{IX}}\left(\frac{x_i}{(x_{\mathrm{Li}}}\right)^{n_i}(y_{\mathrm{Li}}^{\mathrm{IX}})^{n_i} \quad \text{(Ion exchange site)} \qquad (7a)$$

and

$$y_i^{\mathrm{Occ}} = K_i^{\mathrm{Occ}}\left(\frac{x_i}{(x_{\mathrm{Li}}}\right)^{n_i}(y_{\mathrm{Li}}^{\mathrm{Occ}})^{n_i} \quad \text{(Occlusion site)} \qquad (7b)$$

where the superscripts IX and Occ denote the ion exchange and occlusion sites, respectively. Equations 7a and 7b can be combined to yield the total mole equivalents of species i per unit cell of zeolite at equilibrium (θ_i); the expression is given by:

$$\theta_i = n_i(y_i^{\mathrm{IX}} + y_i^{\mathrm{Occ}}) \qquad (8)$$

where θ_i can be measured experimentally and calculated by using Eq. 2. Equation 8 is subjected to two constraints, which are as follows:

$$y_{\mathrm{Li}}^{\mathrm{IX}} + \sum_{i=1}^{M} n_i y_i^{\mathrm{IX}} = 12 \qquad (9a)$$

and

$$y_{\mathrm{Li}}^{\mathrm{Occ}} + \sum_{i=1}^{M} n_i y_i^{\mathrm{Occ}} = (\theta_T - 12) \qquad (9b)$$

where θ_T is the overall total mole equivalents in both ion exchange and occlusion sites, $\theta_T = \Sigma\theta_i$. The total capacity in the framework sites is fixed at 12 equivalents per pseudo unit cell, as is apparent from the molecular formula. But the capacity in the occluded sites is variable due to the differing sizes of the various cations. For example, more LiCl ions can be accommodated in the occluded sites than CsCl ions.

It is important to note that this suggested model should not be used to predict the ion sieving effect commonly encountered with zeolites nor is it affected by this effect. Each of the ions that needs to diffuse into the zeolite's alpha cages has an ionic diameter (see Table 2) less than the pore diameter for zeolite-4A (0.42 nm). Unlike aqueous systems, there are no waters of hydration to make the effective ion size larger. And due to the density of ions in a molten salt, it can be assumed that a cation can diffuse through the pore without dragging a chloride ion with it. Even if the narrow pore size does introduce diffusion rate limitations, this is not relevant to the proposed model, which assumes equilibrium has been established.

Data Preparation and Solving Routine

Only data obtained from Lexa and Johnson[6] had been used to test the monovalent ion exchange model.[7] But for the current proposed model, data from both Lexa and Johnson[6] and Lexa[10] were used. In the earlier publication, the results of salt/zeolite equilibrium experiments involving Li^+, K^+, Cs^+, Rb^+, and Na^+ were reported. In the later publication, results of ion exchange experiments involving additional cations, Sr^{2+} and U^{3+}, were reported. All data were presented in terms of weight percent. Therefore, prior to the analysis, the values in the salt and zeolite phases were converted to mole fraction and moles equivalents per unit cell, respectively.

To solve Eqs. 7-9 and determine best fit values for the equilibrium constants, values of K_i^{IX} and K_i^{Occ} should be initially guessed. Since lithium is chosen as the reference species, the values of $K_{\mathrm{Li}}^{\mathrm{IX}}$ and $K_{\mathrm{Li}}^{\mathrm{Occ}}$ may be set to the value of 1. Then, $y_{\mathrm{Li}}^{\mathrm{IX}}$ and $y_{\mathrm{Li}}^{\mathrm{Occ}}$ can be calculated using Eqs. 9a and 9b. Generally, for monovalent cations, the solutions for both $y_{\mathrm{Li}}^{\mathrm{IX}}$ and $y_{\mathrm{Li}}^{\mathrm{Occ}}$ can be determined easily. Likewise, for the divalent cations, the equations become quadratic and can be easily solved. For trivalent cations, the equations are cubic and are usually considered to be too difficult to solve without numerical techniques. However, there is an algebraic technique that can be used, thus avoiding the need to solve the equations numerically. The principal advantage to this approach is that it saves time for the researcher, since no custom code needs to be written. Once this algebraic technique is employed, the values of y_i^{IX} and y_i^{Occ} can be calculated and added together using Eq. 8. The difference between the value obtained from the model and that from the experimental data can then be determined, and the sum of all errors should be minimized using the least-squares method. New values of K will be automatically guessed at each iteration until the sum of all errors is below the given tolerance using the Newton's method. An example calculation using Sr^{2+} as the surrogate fission species is shown in Figure 1.

Results and Discussion

Comparison to Simpson's monovalent and Gougar's multivalent models

The resulting values of K_i^{IX} and K_i^{Occ} using the least-squares technique from all the data sets are listed in Table 3 and are compared to the previously published values.[7] An alternative

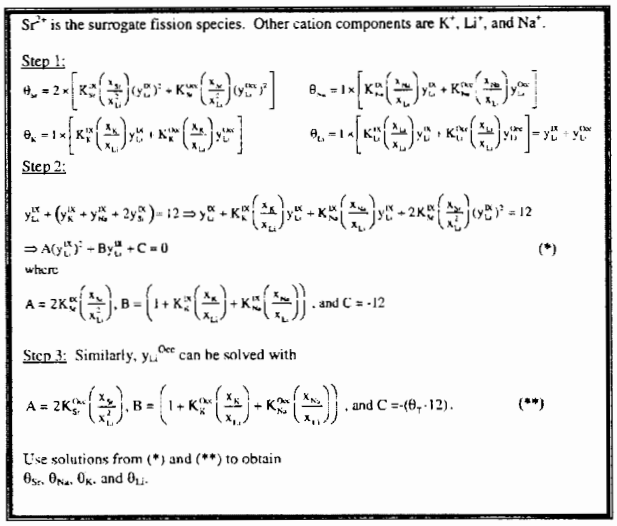

Figure 1. An example calculation of Sr^{2+} as the surrogate fission species.

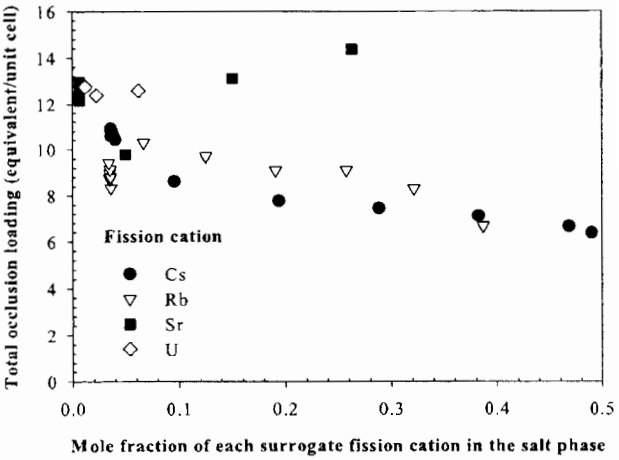

Figure 2. Effect of surrogate fission cation concentration on the total occlusion loading.

formulation of the multicomponent model was reported by Gougar[8]:

$$\theta_i = \frac{S_1 K_i^{IX} C_{i,s}^{1/n_i}}{K_i^{IX} C_{i,s}^{1/n_i} + (1 - C_{i,s})^{1/n_i}} + \frac{S_2 K_i^{Occ} C_{i,s}^{1/n_i}}{K_i^{Occ} C_{i,s}^{1/n_i} + (1 - C_{i,s})^{1/n_i}} \quad (10)$$

where $C_{i,s}$ is the mole equivalent fraction of species i in the salt phase, S_1 is 12, and $S_2 = \theta_T - 12$ was fitted to the same data sets as was the current model. The result is also presented in Table 3 for comparison. It is important to point out that the first and second terms on the RHS of Eq. 10 represent ion exchange and occlusion sites, respectively. From a general observation, depending on the distribution of cations in the zeolite, S_2 or "total occlusion loading" varied from 6.4 to 15 moles per mole of unit cells. The low values came from the presence of high concentrations of either Cs^+ or Rb^+ in the equilibrium system (see Figure 2), showing that the zeolite cage volume is limited according to the ionic radii of Cs^+ (0.169 nm) and Rb^+ (0.148 nm). With additional Cl^- ions in divalent and trivalent species, S_2 values are expected to decrease rapidly as the fission concentrations in the salt phase increase.[10] However, Figure 2 shows that this is not the case because concentrations of U have no significant effect on S_2 and S_2 increases as Sr concentration increases.

It can be seen that the results for the current model and that of Simpson and Gougar[7] closely track each other. This is to be expected since they are based on the same mechanistic concept of two sites with balanced adsorption/desorption rates. Differences in the values may simply come from the fact that there is more data available for the current model with the inclusion of divalent and trivalent data. Before comparing the values of the current model to those of Gougar,[8] it is important to note that the value of K_i in Gougar's work is defined as $K_i = (k_{f,i}/k_{r,i})^{1/n_i}$. After raising the values of K_i by the power of n_i, the comparison between the current model and that of Gougar[8] shows that several of the constants differed between the two models by at least a factor of 9. To make it easier to see how each model predicts relative selectivities, selectivity sequences are given below for the three models.

Current model:

$Sr^{2+} > Li^+ > U^{3+} > Na^+ > K^+ > Cs^+ > Rb^+$ (ion exchange site)

$Cs^+ > Rb^+ > Li^+ > Na^+ > K^+ > U^{3+} > Sr^{2+}$ (occlusion site)

Table 3. Optimal Values for K_i^{IX} and K_i^{Occ} Fitted Through Data from Refs. [6] and [10]

		K_i^{IX}			K_i^{Occ}		
i (# of ion)	Species	Current Model	Simpson and Gougar (2003)	Gougar (2004)*	Current model	Simpson and Gougar (2003)	Gougar (2004)*
1 (+1)	Cs	*0.057*	0.058	0.10 (0.10)	*4.9*	5.4	5.6 (5.6)
2 (+1)	Na	*0.32*	0.32	0.34 (0.34)	*0.92*	0.77	1.3 (1.3)
3 (+1)	Li	*1*	1	8.9 (8.9)	*1*	1	0.34 (0.34)
4 (+1)	K	*0.26*	0.18	0.48 (0.48)	*0.62*	0.83	0.21 (0.21)
5 (+1)	Rb	*0.024*	0.15	0.14 (0.14)	*2.3*	2.0	2.2 (2.2)
6 (+2)	Sr	*1.78*	---	4.6 (21.1)	*0.0000017*	—	0.054 (0.0029)
7 (+3)	U	*0.89*	—	1.5 (3.11)	*0.040*	—	1.2 (1.9)

*The value of K_i in Gougar's work (Ref. [8]) is defined as $K_i = (k_{f,i}/k_{r,i})^{1/n_i}$. The actual $(K_i)^{n_i}$ is given in the parentheses.

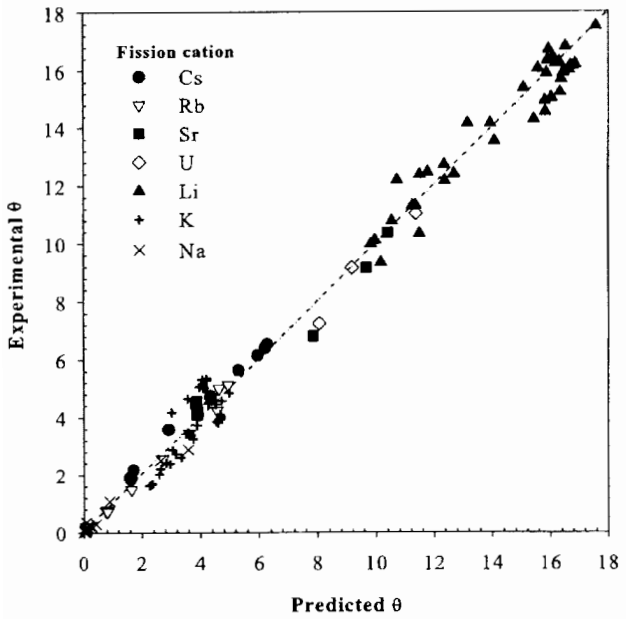

Figure 3. Experimental vs. predicted zeolite loadings (Eq. 8, "current model") for data sets of Refs. 6 and 9.

Simpson and Gougar[7]:

$Li^+ > Na^+ > K^+ > Rb^+ > Cs^+$ (ion exchange site)

$Cs^+ > Rb^+ > Li^+ > K^+ > Na^+$ (occlusion site)

Gougar[8]:

$Sr^{2+} > U^{3+} > Li^+ > K^+ > Na^+ > Rb^+ > Cs^+$ (ion exchange site)

$Cs^+ > Rb^+ > U^{3+} > Na^+ > Li^+ > K^+ > Sr^{2+}$ (occlusion site)

Five general features can be observed from the above comparison. First, it is suggested that Sr^{2+} has the best selectivity in the ion exchange site. However, it is least preferred in the occlusion site. Second, Cs^+ is the best choice of cations in the occlusion site while it is the worst choice in the ion exchange site. This outcome confirms the geometric argument based on the available zeolite cage volume with respect to the size of the ionic cations for the monovalent species. Third, divalent and trivalent species are more preferred in the ion exchange site than the monovalent species with the exception of Li^+. Fourth, the overall scheme (by ranking) indicates that Li^+ is most preferred when both ion exchange and occlusion sites are considered. Fifth, the result indicates that there is a possible way of removing sodium from the ion exchange process. Sodium removal is deemed important, since there is more sodium in the fuel than any fission product and its accumulation in the salt is expected to increase the salt's melting point.

The accuracy of fit is shown in Figure 3, which compares the predicted θ from the current model to the experimental θ measured by Lexa. It is readily apparent that the current model fits the given data very well, properly accounting for multivalent cations. A similar plot is shown in Figure 4 using Gougar's model. Figure 4 illustrates that the model fits both Sr^{2+} and U^{3+} data well and is comparable to the current model (as shown in Figure 3). However, upon careful inspection, the scattered groups of data sets for Li^+ are all coming from Rb^+, Sr^{2+}, and U^{3+} experiments. That is, Eq. 10 overpredicted the θ_{Li} values for the U^{3+} experiment, while it underpredicted those for the Rb^+ and Sr^{2+} experiments. These errors are highlighted in Figure 4 and are suspected to occur because the model only accounts for the mole equivalent fraction of species i in the salt phase (that is, one-dimensional domain).

The difference between the current model and that reported by Gougar is the accountability of interaction of different cation species within the system at equilibrium. Careful analysis reveals that Gougar's model has a limitation of estimating K-values for involved cation species i at low concentrations. For $C_{i,s} \ll 0.1$, this implies that both $K_i^{IX} C_{i,s}^{1/n_i}$ and $K_i^{Occ} C_{i,s}^{1/n_i} \ll 0.1$. Thus, Eq. 10 can be simplified to:

$$\theta_i = C_{i,s}^{1/n_i}(S_1 K_i^{IX} + S_2 K_i^{Occ}) \qquad (11)$$

In a monovalent system, Eq. 11 is simply a linear equation with a constant coefficient. Both K_i^{IX} and K_i^{Occ} will be randomly estimated independently from the other cation species in the system. This is the shortcoming of the model if the species of interest have low concentrations, because the estimated K-values may not be truly representative without considering the influence of other cation species.

Comparison to two-site Langmuir model

Another type of model that is generally used to describe the ion exchange process is based on the Langmuir equation. Typically, the Langmuir equation is applied to the adsorption of molecules on a surface monolayer.[5] The interpretation is of a Type I isotherm, which is what zeolites exhibit. Therefore, the Langmuir model of two-sites ion exchange for monovalent cation species can be given by:

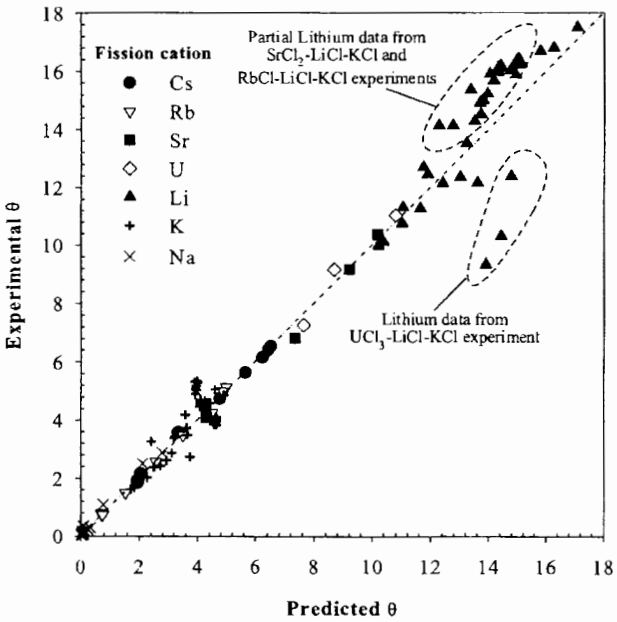

Figure 4. Experimental vs. predicted zeolite loadings (Eq. 10, "Gougar's model") for data sets of Refs. 6 and 9.

Table 4. Optimal Values for k_i^{IX} and k_i^{Occ} for the Two-Site Langmuir Model

i	Species	k_i^{IX}	k_i^{Occ}
1	Cs	115	3,200
2	Na	2,000	0
3	Li	1,800	650
4	K	650	500
5	Rb	200	1,200
6	Sr	0	18,900
7	U	52	24,000

$$\theta_i = \frac{12k_i^{IX}x_i}{1 + \sum_i k_i^{IX}x_i} + \frac{(\theta_T - 12)k_i^{Occ}x_i}{1 + \sum_i k_i^{Occ}x_i} \quad (12)$$

where coefficient k_i^{IX} and k_i^{Occ} are the constants for species i in ion exchange and occlusion sites, respectively. Here x_i is the mole equivalent fraction of species i in the salt phase. It should be mentioned that the value one in the denominator of Eq. 12 indicates that both sites may not be completely occupied. Although Eq. 12 is based on a monovalent cation approach, it is also being used to test the divalent and trivalent species to determine the feasibility and to compare with the current model. The k-values for the Langmuir model are listed in Table 4, and the accuracy of fit is shown in Figure 5. Interestingly, the model fits well with the uranium data sets, while it fails to predict realistic θ values for strontium data. The model overpredicts many potassium data values while it underpredicts many lithium data values. These errors typically propagate as the concentration of the fission product cations increases. The boundaries highlighted in Figure 5 are given to show the areas of high percent error. In addition, U^{3+} data used for the calculation are at lower concentrations when compared to other species in its experimental set. In fact, Sr^{2+} data are at higher concentrations relative to U^{3+} concentrations. Since the model does not fit well for Sr^{2+} data sets, this questions the ability of the model to predict the U^{3+} data at higher concentrations. It is also important to inspect the k-values. It is possible to compare the relative sizes of the k-values for each site. The sequence can be listed as follows:

$Na^+ > Li^+ > K^+ > Rb^+ > Cs^+ > U^{3+} > Sr^{2+}$ (ion exchange site)

$U^{3+} > Sr^{2+} > Cs^+ > Rb^+ > Li^+ > K^+ > Na^+$ (occlusion site)

This result reveals that similar sequences and site preferences are found for the monovalent cation species and for the K-values listed in Table 3 for the current model. The great difference can be seen in divalent and trivalent species, which provides opposite prediction of site preferences from the current model. If the divalent and trivalent species are omitted from the above selectivity sequences, it can be seen clearly that the small cation radii are preferable in the ion exchange site and less desired in the occlusion site. Interestingly, the sequences that account for only monovalent species have similar orders to sequences reported by Simpson and Gougar.[7] These observations confirm the fact that the Langmuir model can only be used for monovalent cation species.

Statistical analysis

Besides the general comparison and contrast among these three models, it is important to look at the statistical aspects among them. Although all three models are non-linear in nature, the correlation coefficient R can be calculated based on the linear interpretation between experimental and predicted θ presented in Figures 3-5. The expression of R is given by:

$$R = \frac{N\sum_i(\theta_{exp_i}\cdot\theta_{p_i}) - (\sum_i\theta_{exp_i})(\sum_i\theta_{p_i})}{\sqrt{N\sum_i\theta_{exp_i}^2 - (\sum_i\theta_{exp_i})^2}\cdot\sqrt{N\sum_i\theta_{p_i}^2 - (\sum_i\theta_{p_i})^2}} \quad (12)$$

where the subscripts exp and p denote experimental and predicted values, respectively. To indicate the degree of correlation, a common test of the R value with the probability distribution is derived from an uncorrelated parent population. In this case, a probability $P_c(R, N)$ test is utilized to determine the degree of correlation from N uncorrelated experimental data points. The expression is given by[11]:

$$P_C(R, N) = \frac{1}{\sqrt{\pi}}\frac{\Gamma\left(\frac{v+1}{2}\right)}{\Gamma\left(\frac{v}{2}\right)}\int_{|R|}^{1}(1-x^2)^{(v-2)/2}dx \quad (13)$$

where $\Gamma(k)$ is the gamma function to the factorial function k! extended to non-integral arguments, and $v = N - 2$. If the probability P_c at the given R and N is less than 0.001, then the probability is high that the experimental and predicted values are correlated and that the fit between them is justified. The values of R, R^2, and P_c for each component, individual system,

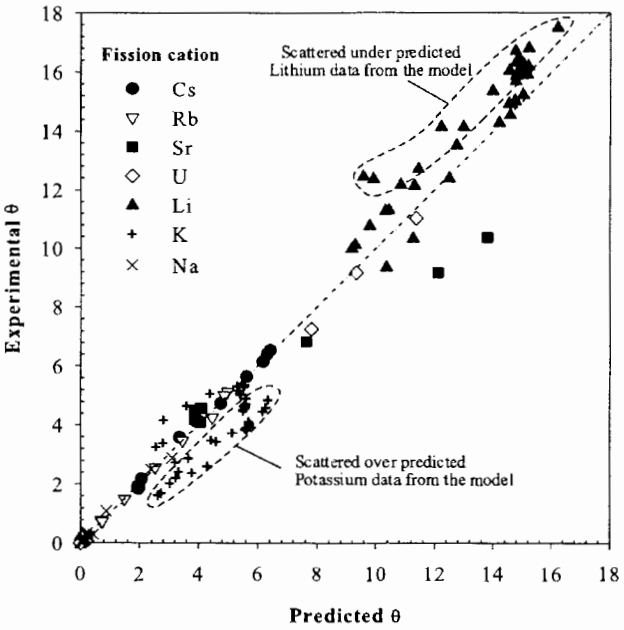

Figure 5. Experimental vs. predicted zeolite loadings (Eq. 11, "two-sites Langmuir model") for data sets of Refs. 6 and 9.

Table 5. Correlation Coefficient (R), Coefficient of Determination (R^2), and Probability Function $P_c(R, N)$ for All Three Models

Model	Current			Gougar (2004)			Langmuir—Two Sites		
System Description	R	R^2	$P_c(R, N)$	R	R^2	$P_c(R, N)$	R	R^2	$P_c(R, N)$
Cs^+	0.998	0.996	5.60E-16	0.999	0.998	2.19E-17	0.999	0.998	1.36E-17
Rb^+	0.995	0.991	6.60E-14	0.998	0.997	1.26E-16	0.998	0.997	3.53E-17
Sr^{2+}	0.986	0.972	1.22E-08	0.994	0.987	3.20E-10	0.997	0.993	1.99E-11
U^{3+}	0.921	0.963	7.64E-04	0.980	0.961	8.28E-04	0.996	0.992	7.63E-05
Na^+	0.988	0.976	1.23E-33	0.990	0.980	4.29E-35	0.993	0.986	2.74E-38
Li^+	0.962	0.925	7.75E-24	0.760	0.578	3.87E-09	0.942	0.887	2.11E-20
K^+	0.781	0.610	8.45E-10	0.796	0.633	2.44E-10	0.741	0.549	1.50E-08
CsCl—LiCl—KCl	0.998	0.997	5.38E-59	0.996	0.992	2.88E-52	0.995	0.989	8.61E-50
RbCl—LiCl—KCl	0.995	0.990	5.68E-48	0.997	0.995	2.81E-55	0.994	0.989	8.08E-49
NaCl—LiCl—KCl	0.999	0.998	9.06E-11	0.999	0.999	3.58E-15	0.988	0.975	6.65E-09
$SrCl_2$—LiCl—KCl	0.996	0.992	2.83E-37	0.994	0.988	1.63E-36	0.971	0.943	2.73E-24
UCl_3—LiCl—KCl	0.990	0.980	3.99E-10	0.960	0.922	2.25E-08	0.991	0.982	3.59E-12
Overall	0.996	0.991	2.74E-160	0.989	0.978	7.51E-129	0.987	0.975	2.41E-124

and overall scheme are calculated for each model and are listed in Table 5 for comparison.

It is apparent that the current model has the highest R value, with $P_c < 0.001$ compared to the other models for an overall system. As expected, the R values for the Li^+ component from both of the latter two models are lower and correspond to the observations in Figures 4 and 5. By carefully reviewing the fit to each component, it can be seen that there is slight non-linear expectation ($R < 0.80$) for all three models. Gougar's model appears to have better linear correlation between the experimental and predicted values for the K^+ data sets than the current and Langmuir models. Yet, it is important, first, to notice that high values of R can be obtained by using a wide range of data, although the data are no more accurate than for a narrow range[11]; and second, not to forget the underlying assumptions in deriving each model even though reported R, R^2, and P_c values for all three models in Table 5 are excellent. Therefore, to provide another meaningful comparison and to distinguish these models in statistical fashion, the residual plots ($\theta_{exp} - \theta_p$) are shown in Figures 6a-6c for all three models. It is evident that Gougar's model under- and overpredicts the experimental Li^+ data at high θ values. This problem also occurs for the Langmuir model, where it underpredicts Li^+ data and overpredicts Sr^{2+} data. Figure 6a shows that the current model has the best capability of predicting the data, as the residual values scattered evenly across the zero line.

Conclusion

A new model has been proposed to predict occlusion and ion exchange between multivalent cation species and zeolite-A in a molten salt. The results reveal interesting outcomes, showing that there is a drastic difference in selectivity for both types of sites. The selectivity of divalent and trivalent species is high in the ion exchange site. However, it is relatively low in the occlusion site. Lithium appears to be the best monovalent cation in the framework site and a moderately good cation in the occlusion site. Cesium appears to have the highest selectivity in the occlusion site. Comparison between the new model and the models presented in the literature reveals that the new model does an excellent job predicting the ion exchange between other multivalent species and zeolite-A. In general, we believe that this modeling technique can be applied to zeolites with other structure types and Si/Al ratios. However, we would expect the equilibrium constants and the total salt loading in the unit cell would be different. Finally, it is hoped that this model will contribute to significant improvement in the design of an ion exchange process for spent nuclear fuel treatment.

Notation

$C_{i,s}$ = mole equivalent fraction of species i in the salt phase, defined in Eq. 10
K = dimensionless equilibrium constant, defined as $K = k_f/k_r$
k_i = constants for species i, defined in Eq. 12
$k_{f,i}$ = forward rate constant of species i
$k_{r,i}$ = reverse rate constant of species i
M = framework charge-balancing cations
MW = molecular weight of species in the zeolite
N = number of experimental data points
n = charge of the exchangeable cations
P_c = probability test, defined in Eq. 14
R = correlation coefficient
S_1 = ion exchange site coefficient, defined in Eq. 10, $S_1 = 12$
S_2 = occlusion site coefficient or total occlusion loading, defined in Eq. 10
v = modified number of experimental data points, defined as $v = N - 2$
$wt\%$ = weight percent of cation species
x_i = mole fraction of species i in the salt phase
y_i = moles of species i per mole of zeolite pseudo unit cells (in the zeolite phase)

Greek letters

$\Gamma(k)$ = gamma function to the factorial function k! extended to non-integral arguments
θ_i = total mole equivalents of species i per unit cell of zeolite at equilibrium
θ_T = overall total mole equivalents in both ion exchange and occlusion sites

Subscripts

exp = experimental values
i = species i
p = predicted or calculated values
S = salt phase
Z = zeolite phase

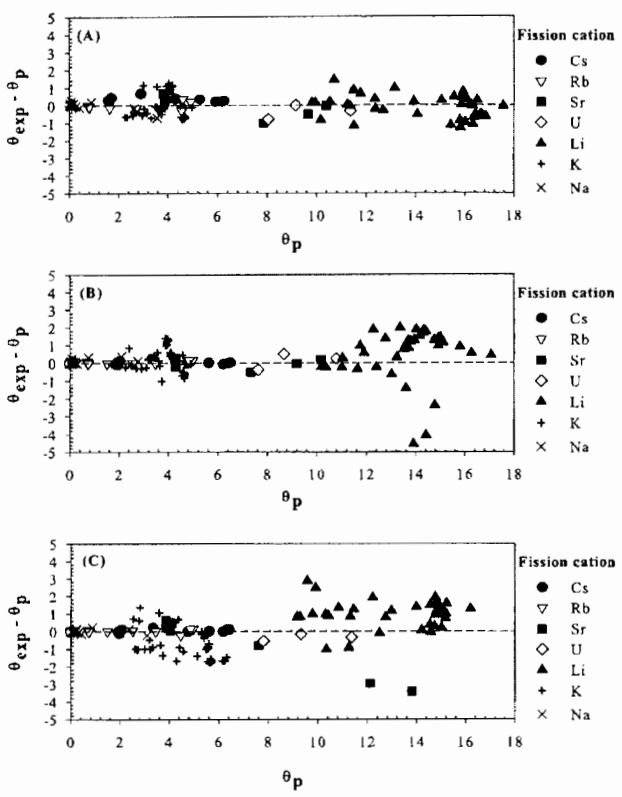

Figure 6. Residual vs. predicted θ for:

(a) Current model, (b) Gougar's model, and (c) Langmuir model.

Superscripts

IX = ion exchange site
Occ = occlusion site

Literature Cited

1. Laidler JJ, Battles JE, Miller WE, Ackerman JP, Carls EL. Development of pyroprocessing technology. *Progress in Nuclear Energy.* 1997;31(1/2):121-140.
2. Benedict RW, McFarlane HF. EBR-II spent fuel treatment demonstration project status. *Radwaste Magazine.* 1998;July:23-28.
3. Simpson MF, Goff KM, Johnson SG, Batemen KJ, Battisti TJ, Toews KL, Frank SM, Moschetti TL, O'Holleran TP. A description of the ceramic waste form production process from the demonstration phase of the electrometallurgical treatment of EBR-II spent fuel. *Nuclear Technology.* 2001;134:263-277.
4. Pereira C, Hash MC, Lewis MA, Richmann MK, Basco J. Incorporation of radionuclides from the electrometallurgical treatment of spent fuel into a ceramic waste form. *Mater Res Soc Symp Proc.* 1999;556: 115-120.
5. Breck DW. *Zeolite Molecular Sieves.* Malabar, FL: Krieger Publishing Company; 1984:530-539.
6. Lexa D, Johnson I. Occlusion and ion exchange in the molten (lithium chloride-potassium chloride-alkali metal chloride) salt + zeolite 4A system with alkali metal chlorides of sodium, rubidium, and cesium. *Metallurgical and Materials Transactions B.* 2001; 32B:429-435.
7. Simpson MF, Gougar MLD. Two-site equilibrium model for ion exchange between monovalent cations and zeolite-A in a molten salt. *Industrial & Engineering Chemistry Research.* 2003;42:4208-4212.
8. Gougar MLD. *Fission Product Ion Exchange Between Zeolite and a Molten Salt.* Ph.D. Diss, Pennsylvania State University; 2004.
9. Reed TB, Breck DW. Crystalline zeolites. II. Crystal structure of synthetic zeolite, type A. *J Am Chem Soc.* 1956;78:5972-5977.
10. Lexa D. Occlusion and ion exchange in the molten (lithium chloride + potassium chloride + alkaline earth chloride) salt + zeolite 4A system with alkaline earth chlorides of calcium and strontium, and in the molten (lithium chloride + potassium chloride + actinide chloride) salt + zeolite 4A system with the actinide chloride of uranium. *Metallurgical and Materials Transactions B.* 2003;34: 201-208.
11. Bevington PR. *Data Reduction and Error Analysis for the Physical Sciences.* New York: McGraw-Hill Book Company; 1969:122-129.